

RESEARCH ARTICLE | MAY 08 2024

Mobile amorphous fraction in polyaryletherketones and its influence on interlayer bonding in material extrusion

Nan Yi ; Richard Davies; Melany McBean; Adam Chaplin; Oana Ghita



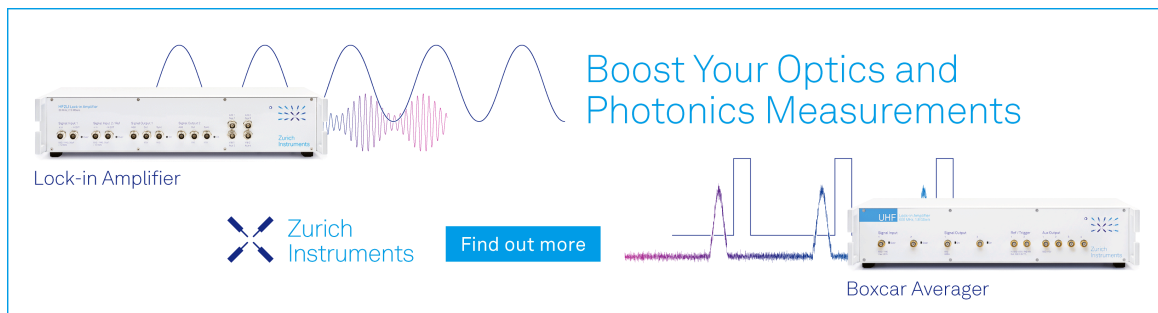
AIP Conf. Proc. 3158, 150002 (2024)

<https://doi.org/10.1063/5.0204567>




12 May 2024 19:34:41

Boost Your Optics and Photonics Measurements



Lock-in Amplifier



Find out more

Boxcar Averager

Mobile Amorphous Fraction in Polyaryletherketones and Its Influence on Interlayer Bonding in Material Extrusion

Nan Yi,^{1, a)} Richard Davies,¹ Melany McBean,¹ Adam Chaplin,² and Oana Ghita¹

¹*Faculty of Environment, Science and Economy, University of Exeter, Exeter, EX4 4QF, United Kingdom*

²*Victrix PLC, Hillhouse international, Thornton Cleveleys, Lancashire, FY5 4QD, United Kingdom*

^{a)}Corresponding author: N.Yi@exeter.ac.uk

Abstract. In general, the mechanical properties of parts manufactured by material extrusion (MEX) process depend upon the interlayer bonding strength. In the case of high temperature polymers such as polyaryletherketones (PAEKs), the printing parameters, in particular the temperatures applied within the process, become a critical factor. The printing-structure-property relationship for these semicrystalline high temperature polymers is complex and not fully understood, often relying on statistical analysis to identify the trends between the processing parameters and the mechanical properties, while missing the microstructural interpretation in between. By controlling the temperature settings and the printing speeds, PAEK parts can be printed in an amorphous state or semicrystalline state. In both cases, molecular chain diffusion at the interface is crucial for achieving good mechanical properties. Using temperature profiles directly determined by the printing parameters, the current work investigates the formation of mobile amorphous fraction (MAF) during printing and its correlation with the correspondent Z tensile strengths. MAF is defined as the fraction of amorphous phase with a higher mobility, which is beneficial to chain diffusion. The conditions required to generate MAF is explored by fast scanning calorimetry (FSC).

The MAF-Z strength correlation is aiming to provide a deeper understanding of the complete processing-structure-property relationships of the MEX process for semicrystalline polymers. It may also provide a microstructural explanation on why slow crystallising PAEK grades are desirable in the MEX process. This study is concentrated on PAEKs which have been printed in an amorphous state to avoid the effect of crystallisation kinetics.

INTRODUCTION

Polyaryletherketones (PAEKs) are a family of high-performance high temperature semicrystalline thermoplastic which are gaining interest in the additive manufacturing (AM) market for demanding applications. Among all the AM technologies, material extrusion (MEX) process is the most widely used one. A major limitation to the full adoption of MEX parts is their anisotropic mechanical properties, usually inferior along the layer deposition direction (i.e. the Z direction). Z tensile strength has been acknowledged as a direct indicator of the layer-to-layer bonding. Hence, weak Z tensile strength entails weak interlayer bonding, mainly caused by poor interlayer diffusion.

In the MEX process, printing parameters are crucial to achieve good interlayer diffusion. However, the microstructural link between interlayer diffusion and the printing parameters is not fully understood and often rely on statistical tools such as design of experiment (DoE) to identify the trends. As an upgrade from the classic two-phase crystalline-amorphous model for semicrystalline polymers, the three-phase model subdivides the amorphous phase into a rigid (RAF) and a mobile amorphous fraction (MAF) [1]. The MAF has a higher molecular mobility and is separated by the lower mobility RAF that arise on the crystalline interface. In theory, a higher amount of MAF is beneficial to chain diffusion. This has been verified by a report on a positive correlation between the MAF and the bond strengths of polyetheretherketones (PEEK) films [2]. Therefore, in this work, we investigated the formation of mobile amorphous phase depending on the printing parameters and its correlation with the corresponding Z tensile strengths. This study sheds light on the missing microstructural link and provides guidance on the parameter selection for maximising interlayer bonding and ultimately the overall mechanical properties.

EXPERIMENTAL

VICTREX AM™ 200 PAEK filaments supplied by Victrix Manufacturing Limited were used for fabricating samples and thermal analyses. Upright tensile bars were printed using a 3DGence Industry F340 according to the five sets of parameters listed in Table 1. Their Z tensile strengths were measured at 5 mm/min by a Shimadzu tensile machine equipped with a 20 kN load cell.

TABLE 1: Printing parameters of the five evaluated set.

Sample condition	ID	Size ^a	Return time (s)	Extrude nozzle temperature (°C)	Build platform temperature (°C)	Build chamber temperature (°C)	Contour velocity (mm/s)	Hatching velocity (mm/s)	Layer thickness (mm)
printed amorphous tested amorphous	1-1	1BA	15.8	390	90	75	20	20	0.3
	1-2		9.1	370	110	55	40	40	
printed amorphous tested annealed	2-1	1A	34	380	100	60	20	30	0.15
	2-2		38.5	390	90	85	20	20	
	2-3		38.5	410	110	85	20	20	

^a Tensile bars were printed according to ISO 527-2.

For each set of parameters, a double-wall structure was created for recording the temperature profiles of selected layers during printing. This simplification was necessary in order to capture clear temperature profiles. The length of the double-walls was adjusted according to the printing velocities to match the layer return times used in the fabrication of the corresponding tensile bars.

Thermal measurements were taken using an Optris Xi400 IR camera and recorded on the Optris PIX Connect software. To ensure accurate and consistent measurements, the camera was placed on the build platform and securely mounted on a custom-printed stand, as shown in Fig. 1(a). Prior to recording, the camera was aligned and focused to the printing location. Temperature measurements were taken at a frame rate of 20 Hz, starting from the beginning of a new layer and ending after 10 peaks were recorded. A peak represents the temperature surge when the nozzle passes the measuring area. In order to record the temperature profile of a specific layer, a measurement area of 1×1 pixels with an emissivity of 1.1 (PAEK) was placed on the centre of the initial layer being recorded, as shown in Fig. 1(b). The emissivity of PAEK was determined by using a thermocouple as the reference, and adjusting the emissivity of the IR camera until the recorded temperature matched the thermocouple. The measurement area was kept fixed for the duration of the recording.

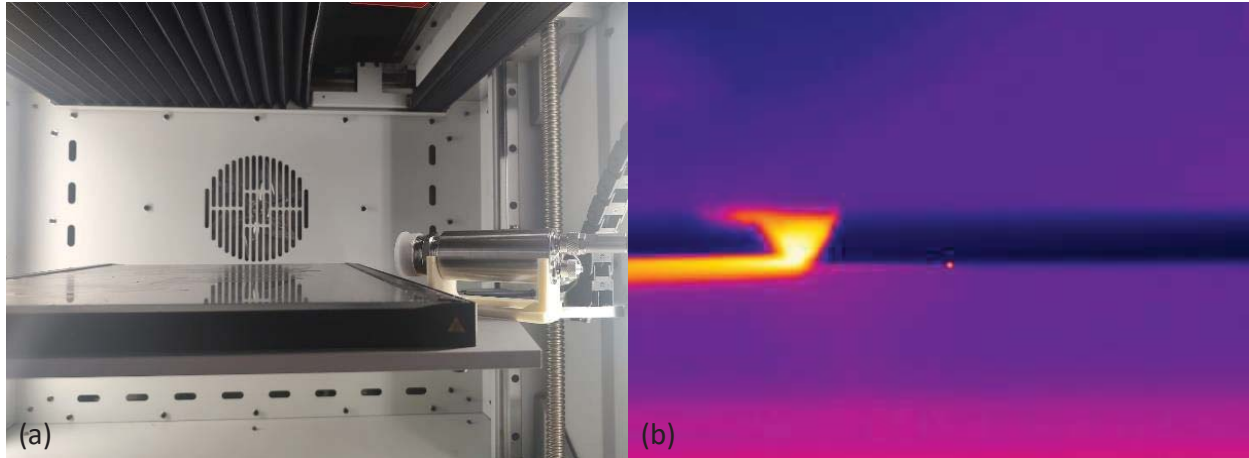


FIGURE 1: (a) Apparatus setup of the IR camera within the 3D printer. (b) Measure area location for first layer measurement.

Thermal analyses were performed on a Mettler Toledo Flash DSC 2+ with UFS 1-type chip sensors. The procedures for sample preparation is described in [3]. All the measurements comprised of a) one heating ramp at $1000 \text{ }^\circ\text{C/s}$ to $400 \text{ }^\circ\text{C}$ to erase the thermal history, b) one cooling ramp at varied cooling rates to $30 \text{ }^\circ\text{C}$, and c) one subsequent heating

ramp at 2500 °C/s to 400 °C to capture the kinetic change around the glass transition temperature T_g . The high heating rate was employed to exclude any recrystallisation during the melting process. The MAF at T_g is calculated from the ratio of heat capacity variation of the semi-crystalline sample $\Delta C_{p,sc}$ to that of the fully amorphous sample $\Delta C_{p,a}$ [2]:

$$\chi_{MAF}(T_g) = \frac{\Delta C_{p,sc}}{\Delta C_{p,a}} \quad (1)$$

RESULTS AND DISCUSSIONS

Conditions for generating MAF

As shown in Fig. 2(a), the step changes in heat capacity at the glass transition vary with the cooling rate. An increase in the step change is attributed to an increase in MAF and a decrease in RAF, since RAF is the solid fraction that does not thermally contribute to the phase change. The MAF formed at each cooling rate was calculated using Equation 1 and plotted in Fig. 2(b). The critical cooling rate for generating 100 % MAF was identified to be above 2 °C/s. Cooling rates slower than this may result in the formation of certain amounts of RAF, potentially hindering the molecular diffusion.

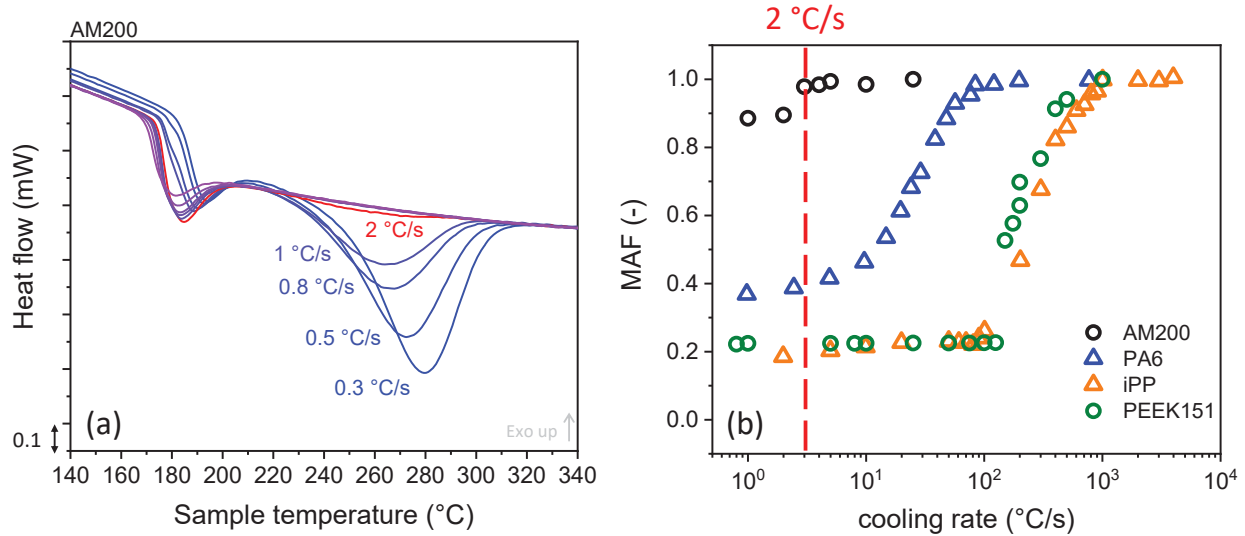


FIGURE 2: (a) Heat flow as a function of temperature in the subsequent heating ramp after cooling at varied rates. (b) MAF as a function of cooling rate, polyamide 6 (PA6) [4], PEEK151 and isotactic polypropylene (iPP) [5] values were added for comparison.

Temperature profiles during printing

In-situ IR imaging was used to acquire the temperature, with one example given in Fig. 3(a). The camera was mounted on the build platform, allowing the temperature evolution of a specific layer to be tracked by fixating the measuring pixel while additional layers were deposited above it. Fig. 3 (b) to (f) illustrate the rapid heating and cooling cycles that occur during the deposition of the layer and subsequent layers. To provide a comprehensive analysis, ten peaks were included for each set of parameters evaluated, as listed in Table 1.

When depositing a single layer with two parallel tracks, typically the temperature profile exhibits two distinct peaks. Fig. 3 (b) to (f) illustrate that the peak with a higher maximum temperature represents the deposition of the front track, while the peak with a lower maximum reflects the deposition of the rear track. After the fourth peak, the maxima of the temperature peaks gradually level off.

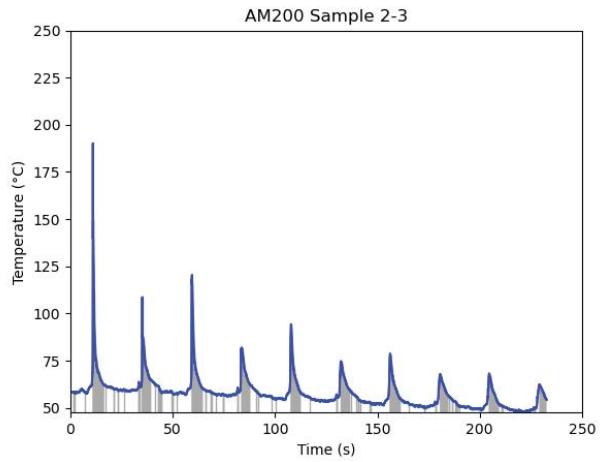
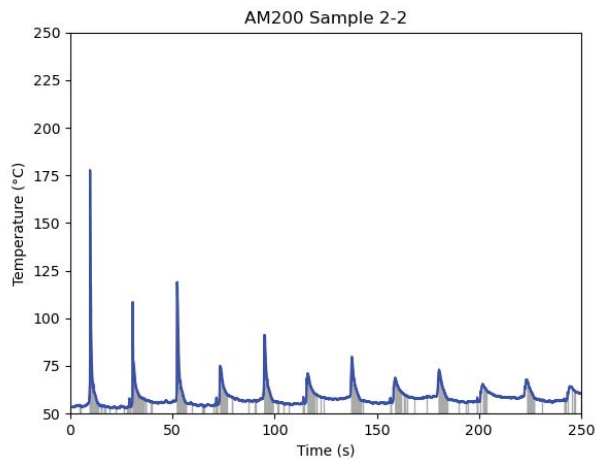
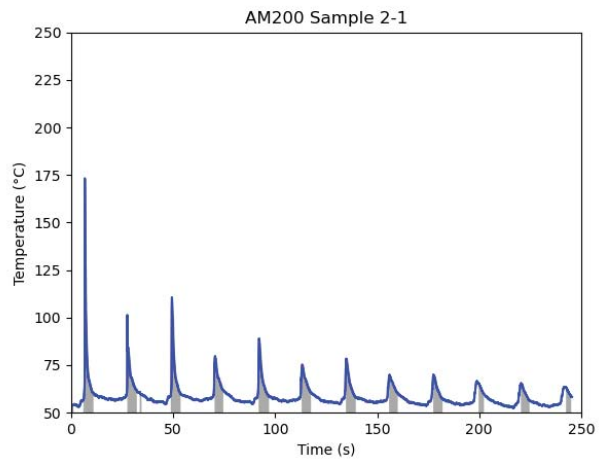
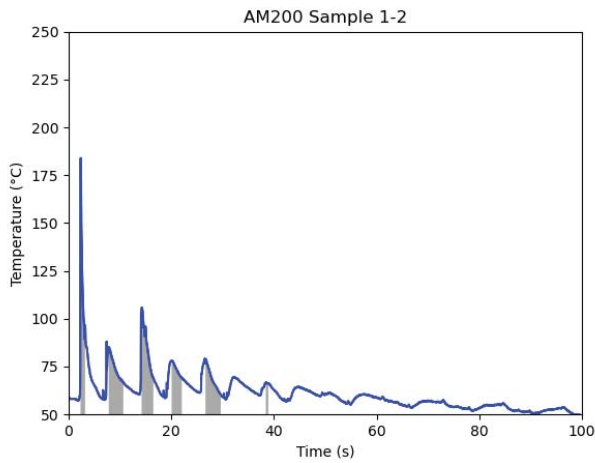
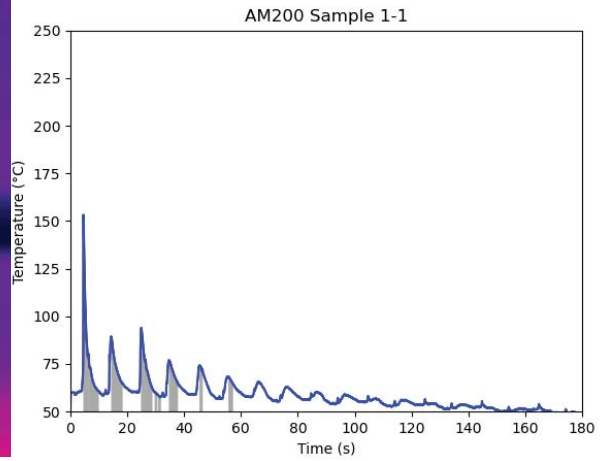
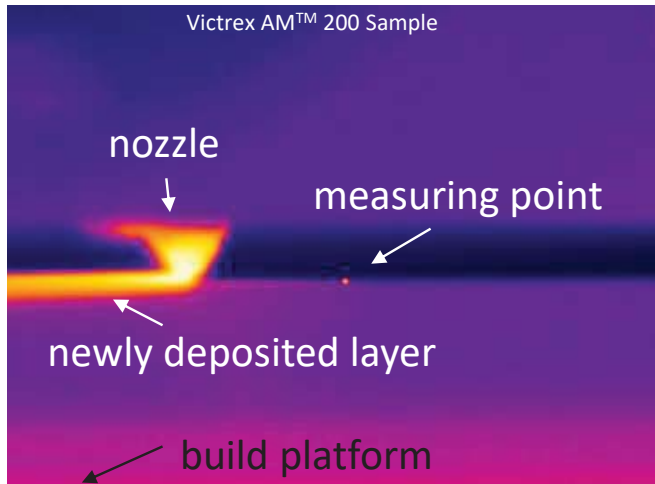


FIGURE 3: Top left: Snapshot from the IR camera capturing the temperature profile of sample 1-1. Graphs: Temperature profiles during the printing of five sets of parameters, according to sample ID listed in Table 1. The shaded areas represent time intervals with a cooling rate faster than 2 °C/s.

TABLE 2: The tensile strengths and the Effective Times of the five evaluated set.

Sample condition	Sample ID	Size ^a	Tensile strength (MPa)	Effective Time (s)
printed amorphous tested amorphous	1-1	1BA	30.2	15.91
	1-2		9.92	9.85
printed amorphous tested annealed	2-1	1A	26	36
	2-2		57.1	44.8
	2-3		58.3	46.5

^a Tensile bars were printed according to ISO 527-2.

MAF-Z strength correlation

As demonstrated in Fig. 3, the cooling rate in any temperature profile constantly changes. It is identified in Fig. 2 that there is a critical cooling of 2 °C/s for generating 100 % MAF. The time intervals $t_{critical,i}$ during which the cooling rate was faster than this critical cooling rate were identified and highlighted in Fig. 3. The sum of these time intervals for each set of parameters was calculated according to Eq. 2 and termed as the Effective Time $t_{effective}$, during which 100 % MAF should be generated. The Effective Times are summarised in Table 2.

$$t_{effective} = \sum_{i=1}^n t_{critical,i} \quad (2)$$

A longer Effective Time results in higher MAF and lower RAF generation. As a higher MAF promotes molecular diffusion, it leads to higher interlayer bonding strength. The strength of these interlayer bonds can be evaluated using Z-strength. Accordingly, a positive correlation between the Z-strength and the Effective time is expected, which is confirmed by the results presented in Table 2. The correlation between Effective Time and Z-strength is currently valid only for sets with same geometry and printing conditions. In this case, tensile test type specimens were used. Further investigation is required to compare the results across different geometries and printing conditions and confirm whether such a method holds as a general rule and relationship between print Effective Time and Z strength.

In Fig. 2, AM200 exhibits a slower critical cooling rate compared to PA6, iPP, and PEEK151. This implies that, with similar temperature profiles, the Effective Time of AM200 is significantly longer compared to, for example, PEEK151. As a result, AM200 is capable of generating a greater amount of MAF during the printing process, promoting interlayer diffusion and leading to stronger interlayer bonding. Ultimately, these characteristics contribute to superior mechanical properties, particularly in the Z direction.

The generation of MAF can also explain the increased difficulty in printing PP [6] compared to PEEK151. Fig. 2 illustrates that PP and PEEK151 possess similar critical cooling rates. However, the melting temperature of PP is considerably lower, resulting in much lower thermal gradient during printing compared to PEEK. Consequently, during printing PP generates significantly less amount of MAF compared to PEEK, resulting in reduced diffusion which leads to weaker interlayer bonding and delamination in the printed PP parts.

CONCLUSION

This study presents a methodology to evaluate the amount of MAF generated during the printing process of semi-crystalline polymers. The findings demonstrate a positive correlation between the amount of MAF generated and the interlayer bonding strength in high-temperature semicrystalline polymers. The identification of a critical cooling rate to generate high MAF suggests a missing microstructural link between printing parameter settings and final mechanical properties. While this study was conducted on PAEKs, its conclusions may be broadly applicable to other semicrystalline polymers as well. These findings can guide the selection of printing parameters and potentially be used to tune the properties of final printed parts in the future.

REFERENCES

1. B. Wunderlich, "Reversible crystallization and the rigid-amorphous phase in semicrystalline macromolecules," *Progress in Polymer Science (Oxford)* **28**, 383–450 (2003).
2. F. Awaja and S. Zhang, "Self-bonding of PEEK for active medical implants applications," *Journal of Adhesion Science and Technology* **29**, 1593–1606 (2015).
3. N. Yi, R. Davies, A. Chaplin, P. McCutcheon, and O. Ghita, "Slow and fast crystallising poly aryl ether ketones (PAEKs) in 3D printing: Crystallisation kinetics, morphology, and mechanical properties," *Additive Manufacturing* **39**, 101843 (2021).
4. E. Parodi, L. Govaert, and G. Peters, "Glass transition temperature versus structure of polyamide 6: A flash-DSC study," *Thermochemica Acta* **657**, 110–122 (2017).
5. J. E. Schawe, "Analysis of non-isothermal crystallization during cooling and reorganization during heating of isotactic polypropylene by fast scanning DSC," *Thermochemica Acta* **603**, 85–93 (2015).
6. O. S. Carneiro, A. F. Silva, and R. Gomes, "Fused deposition modeling with polypropylene," *Materials and Design* **83**, 768–776 (2015).